Testing the self-consistent renormalization theory for the description of the spin-fluctuation modes of MnSi at ambient pressure

2005 J. Phys.: Condens. Matter 17 L129

(http://iopscience.iop.org/0953-8984/17/13/L01)

INSTITUTE OF PHYSICS PUBLISHING JOURNAL OF PHYSICS: CONDENSED MATTER

J. Phys.: Condens. Matter **17** (2005) L129–L135 doi:10.1088/0953-8984/17/13/L01

LETTER TO THE EDITOR

Testing the self-consistent renormalization theory for the description of the spin-fluctuation modes of MnSi at ambient pressure

A Yaouanc[1], P Dalmas de Réotier[1], P C M Gubbens[2], S Sakarya[2], G Lapertot[1], A D Hillier[3] and P J C King[3]

[1] CEA/DSM/Département de Recherche Fondamentale sur la Matière Condensée, F-38054 Grenoble cedex 9, France
[2] Department of Radiation, Radionuclides and Reactors, Faculty of Applied Sciences, Delft University of Technology, 2629 JB Delft, The Netherlands
[3] ISIS Facility, Rutherford Appleton Laboratory, Chilton, Didcot OX11 0QX, UK

Received 6 January 2005, in final form 4 March 2005
Published 18 March 2005
Online at stacks.iop.org/JPhysCM/17/L129

Abstract
We report positive muon spin measurements of the spin–lattice relaxation rate, λ_Z, for the weakly helimagnetic metal MnSi performed at ambient pressure and covering the temperature range from 2 to 280 K. The self-consistent renormalization theory is unable to explain the temperature dependence of λ_Z, in particular far below the ordering temperature and in the critical paramagnetic regime. A temperature independent length scale is required to account for these data.

(Some figures in this article are in colour only in the electronic version)

The weakly helimagnetic metal MnSi is becoming the model system for the investigation of anomalous metallic properties. Thanks to recent developments of physical measurements under high pressure, anomalous properties have been detected over a wide region of its phase diagram near the pressure-induced first-order magnetic–non-magnetic transition [1]. More surprisingly, even at ambient pressure the expected metallic behaviour is not observed with the optical conductivity [2].

Here we report an investigation of the spin dynamics by the muon spin relaxation (μSR) technique; for references to this technique see e.g. [3–5]. It confirms that at ambient pressure the physical properties of MnSi are still not understood: we find the predictions of the conventional theory for a weakly magnetic metal, i.e., the self-consistent renormalization (SCR) theory [6], at variance with the experimental results in a large temperature range. These results are explained if a new length scale is introduced.

MnSi is a metallic compound which undergo a second order magnetic phase transition at $\sim$29.5 K into a helical magnetic structure characterized by a small wavevector $Q_0 = 0.035$ Å^{-1}

parallel to [111] or equivalent crystal directions [7]. The magnetic moments lie in planes perpendicular to $\mathbf{Q}_0$ and their magnitude, extrapolated to $T = 0$ K, is $M_{Q_0} = 0.4\ \mu_B$. The uniform magnetic susceptibility χ_0 follows a Curie–Weiss law up to 400 K [8]. MnSi is particularly attractive experimentally because of the possibility to produce large high quality crystals. With its three-dimensional cubic crystal structure (B20 lattice type with space group $P2_13$), the electronic and magnetic properties of MnSi can be assumed to be isotropic.

We first review the predictions of the SCR theory or the equivalent Ginzburg–Landau expansion [9]. As usually done, we shall first neglect the long-range modulation and therefore assume MnSi to be a weak ferromagnet. The static wavevector dependent susceptibility in the paramagnetic state is of the Ornstein–Zernike form in the whole Brillouin zone, i.e. $\chi_0(q) \propto (q^2 + \kappa^2)^{-1}$. q is referred relative to the zone centre. κ is the inverse of the correlation length of the magnetic modes which follows the power law $\kappa(T) = \kappa_0[(T - T_c)/T_c]^{\nu}$. The exponent ν is expected to be mean-field-like, that is $\nu = \nu_{MF} = 1/2$. T_c is the critical temperature. The relaxation rate of a spontaneous spin-fluctuation takes the form $\Gamma_0(q) \propto q\chi_0^{-1}(q) \propto q(\kappa^2+q^2)$. The linear decay at small q is known as Landau damping. The spin–lattice relaxation rate, denoted $1/T_1$ in nuclear magnetic resonance and λ_Z in μSR, can be expressed as a sum over the Brillouin zone; see e.g. [5]. Assuming that there is no applied magnetic field on the sample,

$$\lambda_Z(T) \propto T \int_{q_\ell}^{q_u} \frac{\chi_0(q)}{\Gamma_0(q)} q^2\,\mathrm{d}q. \tag{1}$$

q_u and q_ℓ are cut-off wavevectors. λ_Z is then found to be proportional to $T\chi_0$ when $q_u/\kappa \gg 1$ [10]. Since χ_0 follows the Curie–Weiss law, in the paramagnetic phase $\lambda_Z(T) \propto T/(T - T_c)$. λ_Z is therefore expected to diverge at T_c and to level off for $T \gg T_c$. Deep in the ordered state, the perpendicular (to the easy axis) spin fluctuations are expected to be stronger than the parallel ones and therefore we need only to consider $\chi_0^{\perp}(q)$ and $\Gamma_0^{\perp}(q)$ [6]. Because of the Goldstone mode, $\chi_0^{\perp}(q) \propto q^{-2}$, and therefore $\lambda_Z(T) \propto T/q_\ell^2$. Since $q_\ell = k_F^{\uparrow} - k_F^{\downarrow}$, where $k_F^{\uparrow}$ and $k_F^{\downarrow}$ are the Fermi wavevectors for the majority ($\uparrow$) and minority ($\downarrow$) spin electron bands respectively [9], $q_\ell \propto M_0$. Therefore $\lambda_Z(T) \propto T/M_0^2$, as given in [10].

The forms for $\chi_0(q)$ and $\Gamma_0(q)$ in the paramagnetic phase are extensively supported by the results of neutron scattering experiments [11]. However, inspection of these data shows that the measurements were only performed down to $q = 0.1$ Å^{-1}.

Using the same methodology, it is found that $\lambda_Z(T) \propto T/(T - T_N)^{1/2}$ and $\lambda_Z(T) \propto T/M_{Q_0}$ for an antiferromagnet in the paramagnetic and ordered phases respectively [10]. Hence, $\lambda_Z(T) \propto T^{1/2}$ in the high-temperature limit, i.e. λ_Z should never level off at high temperature.

Measurements of $\lambda_Z(T, B_{ext})$ have already been published [12–14]. The available data for the paramagnetic phase at low field are consistent with Moriya's predictions assuming MnSi to be a ferromagnet. However, at least one data point in [13] suggests a saturation occurs when approaching the critical point. In addition, from the same reference we note that the theory may not reproduce λ_Z at high temperature. The measurements reported here were designed to further investigate $\lambda_Z(T)$ at low field.

Referring to the work of Kadono *et al* [13], we chose to apply a longitudinal field B_{ext} of either 5 or 20 mT. B_{ext} is sufficiently weak to neglect its effect on λ_Z [14], outside the field range where a resonance with the ^{55}Mn nuclear magnetic moments occurs, and strong enough to quench the depolarization arising from these moments.

The measurements were performed using the EMU spectrometer of the ISIS facility (UK). The data were recorded between 2 and 280 K in the so-called 'fly-past' mode. Basically, in this mode the muons which miss the sample do not contribute to the measured spectrum.

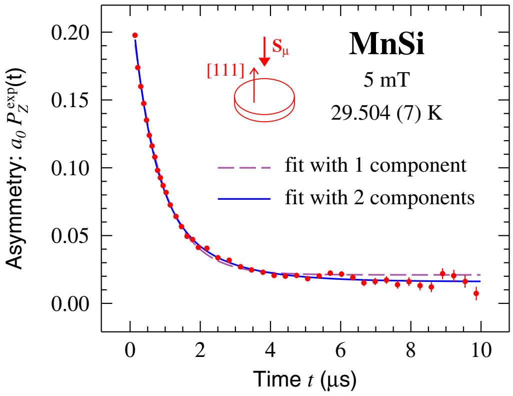

Figure 1. A μSR spectrum recorded in the paramagnetic phase of a single crystal of MnSi. A longitudinal field of 5 mT was applied along the [111] crystal axis. The dashed (full) line is a fit with the one- (two-) component model. These models consist either of a simple exponential ($P_Z(t) = \exp(-\lambda_Z t)$) or of the weighted sum of two exponential functions ($P_Z(t) = p_1 \exp(-\lambda_{Z,1} t) + p_2 \exp(-\lambda_{Z,2} t)$, with $p_1 + p_2 = 1$). The latter model accounts for the two magnetically inequivalent muon sites (with a population ratio $p_2/p_1 = 0.77$ (9)) which are known to exist [16]. The predictions from the two models are slightly different for $t > 2\ \mu$s. $\chi^2 = 1.2$ and 1.9 for the two- and one-component fits, respectively.

A MnSi single crystal was grown from a polycrystalline ingot using the Czochralski method. The residual resistivity ratio is 40 for similarly prepared samples [15]. Crystals with ratios up to 200 have been reported in the literature. However, it has been argued that once the compound has a sufficiently high ratio, as in our case, the magnetic properties are no longer sample dependent [15, 1].

The μSR technique used here gives access to the so-called asymmetry $a_0 P_Z^{\exp}(t)$ where a_0 is the initial muon asymmetry and $P_Z^{\exp}(t)$ the muon polarization function measured along the direction of the initial muon beam polarization, $\mathbf{Z}$. All the spectra were analyzed assuming $a_0 P_Z^{\exp}(t) = a_s P_Z(t) + a_{\rm bg}$. The first term on the right-hand side describes the μSR signal from the sample and the second accounts for the few muons stopped in the background, i.e., the cryostat walls or windows. A typical spectrum recorded close to the critical temperature is presented in figure 1. Since we are here mostly interested in the spin dynamics, the spectra recorded in the ordered phase were analysed with a large binning, so that wiggles arising from the spontaneous field at the two muon sites [16] become invisible and therefore do not have to be modelled. However, close to the critical point the wiggles from the smallest spontaneous field were easily observed. They served to determine the critical temperature through a fit of the temperature dependence of the spontaneous field to a power law using as exponent $\beta = 0.367$ valid for an isotropic magnet. We obtained $T_{\rm c} = 29.460(25)$ K.

The muons probe two magnetically inequivalent interstitial sites [16]. These are resolved near the critical point as shown in the example of figure 1. The analysis of such spectra yields λ_Z as explained in the caption of figure 2. The comparison of the measured λ_Z with the prediction of the SCR theory shows that this theory breaks down in the whole temperature range. λ_Z was found to be approximately temperature independent above 80 K, whereas a decrease was expected for the ferromagnetic model; see figure 2. The failure of the SCR theory is pronounced in the critical paramagnetic region. Interestingly, while our measurements are more precise than previous ones [13], they are entirely consistent, notably in the critical regime. In figure 3 we display $\lambda_Z(T)$ for the magnetically ordered state. Experimentally, $\lambda_Z(T) \propto T$ up

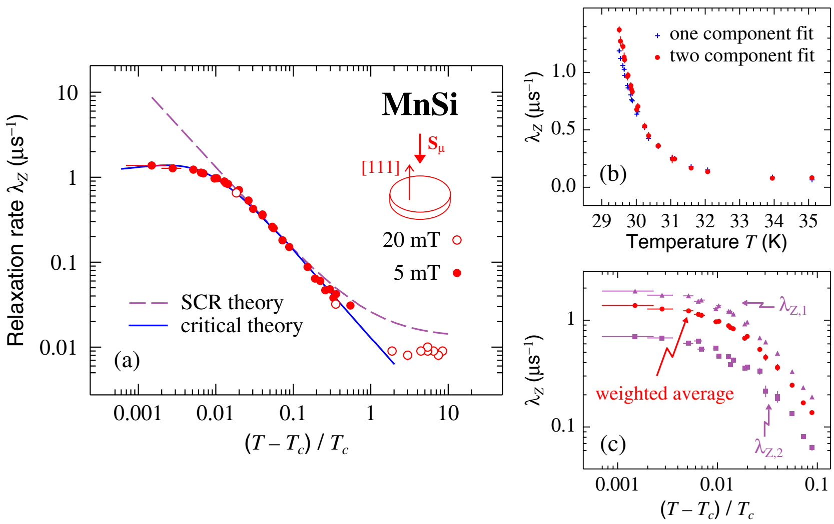

Figure 2. (a) Spin–lattice relaxation rate λ_Z versus the reduced temperature $\tau \equiv (T - T_c)/T_c$ with $T_c = 29.460$ K. A longitudinal field of either 5 or 20 mT was applied along the [111] crystal axis to quench the nuclear fields arising from the ^{55}Mn nuclei [13]. The horizontal and vertical error bars are smaller than the size of the data point except for the point at the lowest temperatures. The dashed line shows the prediction of the SCR theory for the ferromagnetic case with the scale parameters chosen to best fit data satisfying $0.01 < \tau < 1$. The SCR theory for an antiferromagnet would give a worse fit with half the slope for $\tau \lesssim 0.1$ and an increase of λ_Z for $\tau > 1$ ($\lambda_Z \propto T^{1/2}$ in the high-temperature limit). The solid line results from a fit of the data recorded near the critical point using the critical paramagnetic model described in the main text. We find that it is valid at least for $\tau \leqslant 0.4$. (b) Comparison in the region close to T_c between the relaxation rates deduced from the two models used for $P_Z(t)$ (see caption of figure 1). The weighted mean (with relative weights p_1 and p_2) of the two decay rates is plotted in the case of the two-component fit. When the relaxation rate is smaller than 0.5 μs^{-1} the two models yield indistinguishable values. (c) Temperature dependence of the two relaxation rates $\lambda_{Z,1}$ and $\lambda_{Z,2}$ and of their weighted average close to T_c. A saturation near the critical point is apparent for each of them. λ_Z plotted in (a) corresponds to the one-component fit for $\lambda_Z \leqslant 0.5$ μs^{-1} and to the weighted average of $\lambda_{Z,1}$ and $\lambda_{Z,2}$ for the other points.

to ∼22.5 K. As shown in the figure, the SCR theory also breaks down deep in the magnetically ordered state.

First we discuss the saturation of λ_Z in the critical paramagnetic regime. It has already been detected for a number of ferromagnets: Ni [18], Gd [19, 20] and $GdNi_5$ [21]. The saturation is the definitive signature of the influence of the dipole interaction on the critical spin dynamics. Recently λ_Z measured for the ferromagnetic heavy fermion compound UGe_2 has also been found to saturate close to T_c [22]. Interestingly, in this case λ_Z was interpreted as arising from the itinerant electrons and an analogy was drawn between the spectral density of the fluctuations of these electrons and those of weakly ferromagnetic metals.

No saturation of λ_Z is observed for conventional antiferromagnets, see e.g. [23]. Using the value $\kappa_0 = 0.18$ Å^{-1} [11] and $\nu = 1/2$ one deduces that the inverse correlation length of the fluctuations in MnSi already reaches the value of the magnetic structure propagation wavevector for a reduced temperature $\tau \equiv (T - T_c)/T_c \simeq 0.04$. At the temperatures for which λ_Z saturates ($\tau \lesssim 0.015$), MnSi cannot be therefore considered as a ferromagnet. The saturation observed in the λ_Z critical behaviour of a ferromagnet essentially arises from the presence of a length scale $1/q_D$ which, as recalled below, precludes the divergence of the

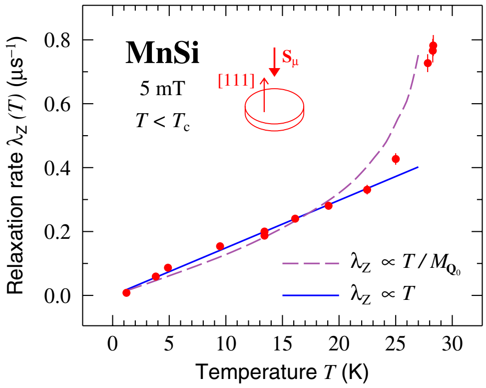

Figure 3. Spin–lattice relaxation rate λ_Z versus temperature measured in the ordered phase of MnSi. A longitudinal field of 5 mT was applied along the [111] crystal axis. The solid line is the result of a linear fit with a slope of 14.9 (1) ms^{-1} K^{-1}. The SCR prediction for the antiferromagnetic case is also shown: $\lambda_Z \propto T/M_{\mathbf{Q}_0}$. The two fits are done for $T \leqslant 22.5$ K and result in $\chi^2 = 1.05$ and 6.75, respectively. The SCR curve has been computed using $M_{\mathbf{Q}_0}$ obtained from neutron scattering [17]. The misfit for the ferromagnetic SCR model is obviously expected to be even worse than for the antiferromagnetic case. That the linear fit breaks down at 25 K and above is not surprising since we are entering the temperature region where the critical spin fluctuations should drive the muon spin relaxation.

longitudinal fluctuation modes. $\lambda_Z(T)$ in MnSi close to T_c suggests therefore the existence of a temperature independent length scale. The physical origin for this length scale in MnSi is not necessarily the same as in ferromagnets for which it follows from the dipolar interaction. In the following part we briefly describe the theory for the critical behaviour of λ_Z in the presence of a temperature independent length scale as in dipolar Heisenberg ferromagnets.

The key point for understanding the saturation of λ_Z for a ferromagnet close to T_c is to notice that only long wavelength fluctuations contribute to the critical dynamics. Hence, in addition to the isotropic exchange interaction, the dipole interaction has to be included due to its long range nature [24]. The wavevector dependent susceptibility is then a tensor, rather than a scalar as assumed in the conventional SCR theory, with elements $\chi^{\alpha\beta}(\mathbf{q}) = \chi^{L}(q)P_{L}^{\alpha\beta}(\mathbf{q}) + \chi^{T}(q)P_{T}^{\alpha\beta}(\mathbf{q})$. $P_L(\mathbf{q})$ ($P_T(\mathbf{q})$) is the longitudinal (transverse) projection operator with respect to wavevector $\mathbf{q}$. For the longitudinal and transverse susceptibilities, $\chi^L(q)$ and $\chi^T(q)$, the Ornstein–Zernike form is used:

$$\chi^{L}(q) = \frac{q_D^2}{q^2 + q_D^2 + \kappa^2} \qquad \text{and} \qquad \chi^{T}(q) = \frac{q_D^2}{q^2 + \kappa^2}. \tag{2}$$

q_D is the dipole wavevector which is a measure of the strength of the exchange interaction relative to the dipole energy [24]. As for the susceptibility, the longitudinal and transverse fluctuation rates have to be distinguished: $\Gamma^{L,T}(q) \propto q^z \hat{\Gamma}^{L,T}(\kappa/q, q_D/q)$ with the critical dynamical exponent $z = 5/2$. $\hat{\Gamma}^{L,T}$ are scaling functions which depend on two scaling variables. $\kappa(T)$ still follows a power law but now with an exponent $\nu = \nu_{cri} \simeq 0.70$. Because we need to distinguish the longitudinal and transverse susceptibilities and fluctuation decay rates, λ_Z is derived to be the sum of two components [25]: $\lambda_Z(T) = \mathcal{W}\left[a_L I^L(T) + a_T(T) I^T(T)\right]$. $I^{L,T}$ are scaling functions obtained from mode–mode coupling theory. As the critical temperature is approached from above, I^T diverges whereas I^L becomes approximately temperature independent for $\kappa/q_D < 1$ [24]. $\mathcal{W}$ is a scale parameter and $a_{L,T}$ are parameters which only depend on the muon site and hyperfine coupling. a_T has always been found to be small relative to a_L. As noticed from figure 2, a good fit of $\lambda_Z(T)$ in the paramagnetic critical regime is obtained with the model we have just sketched. The parameters are $\mathcal{W}a_{\mathrm{L}} = 8.50(26)\ \mu\mathrm{s}^{-1}$ and $q_{\mathrm{D}}/\kappa_0 = 0.022$ (1), setting $a_{\mathrm{T}} = 0$. From the literature one finds $q_{\mathrm{D}} = 6.9 \times 10^{-3}$ Å^{-1} [9] and $\kappa_0 = 0.18$ Å^{-1} [11], therefore $q_{\mathrm{D}}/\kappa_0 = 0.038$ not far from our value.

The saturation of λ_Z near T_{c} arises from the presence, in addition to the correlation length $1/\kappa$, of a temperature independent second length scale, $1/q_{\mathrm{D}}$. q_{D} suppresses fluctuations close to T_{c} near the zone centre. This is clearly seen from the expression of $\chi^{\mathrm{L}}(q)$; see equation (2). Referring to [26], when λ_Z is temperature independent close to T_{c}, the relaxation stems from modes for which $q \leqslant 10\, q_{\mathrm{D}} \simeq 0.07$ Å^{-1}.

In fact, MnSi is characterized by a long-range chiral modulation which is expected to influence the wavevector dependent susceptibility. Since it diverges at T_{c} [27, 28], it cannot explain $\lambda_Z(T)$. Note that λ_Z is diverging at the critical point for conventional antiferromagnets, see e.g. [23]. The absence of divergence of λ_Z in the critical paramagnetic regime strongly suggests a cut-off wavevector such as q_{D} to be at play. A definitive answer requires a theoretical study which has to account for the modulated nature of MnSi.

The linear thermal behaviour of λ_Z for $T \ll T_{\mathrm{c}}$ follows from equation (1) if q_ℓ is assumed to be temperature independent. This means that q_ℓ is not determined by the Fermi wavevectors for the majority and minority spin electron bands, but by a smaller temperature independent wavevector, as already required for understanding the critical spin dynamics.

An effective non-analytical long-range interaction between spin-fluctuation modes has been proposed for MnSi; see [29] and references therein and [30]. This interaction may renormalize the susceptibility. A theoretical investigation of its effect on the spin dynamics is certainly worthwhile.

In conclusion, the SCR theory fails to account for the temperature dependence of the spin–lattice relaxation rate measured by μSR on MnSi. According to our results, at criticality the neutron quasi-elastic linewidth should not follow the q^3 dependence predicted by the SCR theory, but scale as q^z with z close to 2.5 according to mode–mode coupling theory [24]. This behaviour has already been suggested for the weak ferromagnet Ni_3Al [31]. Our present μSR study shows definitively a second temperature independent length scale to be required for the description of the spin dynamics of weak ferromagnets, both in the critical regime and far below the critical temperature.

We are grateful to G Knebel for a discussion on the resistivity measurements, B Fåk for communication of values of M_{Q_0} measured by neutron diffraction prior to publication and M E Zhitomirsky for conversations.

References

[1] Doiron-Leyraud N, Walker I R, Taillefer L, Steiner M J, Julian S R and Lonzarich G G 2003 *Nature* **425** 595
[2] Mena F P, van der Marel D, Damascelli A, Fäth M, Menovsky A A and Mydosh J A 2003 *Phys. Rev.* B **67** 241101(R)
[3] Karlsson E B 1995 *Solid State Phenomena as Seen by Muons, Protons and Excited Nuclei* (Oxford: Clarendon)
[4] Amato A 1997 *Rev. Mod. Phys.* **69** 1119
[5] Dalmas de Réotier P and Yaouanc A 1997 *J. Phys.: Condens. Matter* **9** 9113
[6] Moriya T 1985 *Spin Fluctuations in Itinerant Electron Magnetism* (Berlin: Springer)
[7] Ishikawa Y, Tajima K, Bloch D and Roth M 1976 *Solid State Commun.* **19** 525
[8] Yasuoka H, Jaccarino V, Sherwood R C and Wenick J H 1978 *J. Phys. Soc. Japan* **44** 842
[9] Lonzarich G G and Taillefer L 1985 *J. Phys. C: Solid State Phys.* **18** 4339
[10] Moriya T and Ueda K 1974 *Solid State Commun.* **15** 169
[11] Ishikawa Y, Noda Y, Uemura Y J, Majkrzak C F and Shirane G 1985 *Phys. Rev.* B **31** 5884

[12] Hayano R S, Uemura Y J, Imazoto J, Nishida N, Nagamine K, Yamazaki T, Ishikawa Y and Yasuoka H 1980 *J. Phys. Soc. Japan* **49** 1773
[13] Kadono R, Brewer J H, Chow K, Kreitzman S R, Niedermayer C, Riseman T M, Schneider J W and Yamazaki T 1993 *Phys. Rev.* B **48** 16803
[14] Gat-Malureanu I M, Fukaya A, Larkin M I, Millis A J, Russo P L, Savici A T, Uemura Y J, Kyriakou P P, Luke G M, Wiebe C R, Sushko Y V, Heffner R H, MacLaughlin D E, Andreica D and Kalvius G M 2003 *Phys. Rev. Lett.* **90** 157201
[15] Thessieu C, Flouquet J, Lapertot G, Stepanov A N and Jaccard D 1995 *Solid State Commun.* **95** 707
[16] Kadono R, Matsuzaki T, Yamazaki T, Kreitzman S R and Brewer J H 1990 *Phys. Rev.* B **42** 6515
[17] Fåk B, Sadykov R A, Flouquet J and Lapertot G 2005 *J. Phys.: Condens. Matter* **17** 1635
[18] Nishiyama K, Yagi E, Ishida K, Matsuzaki T, Nagamine K and Yamazaki T 1984 *Hyperfine Interact.* **17–19** 473
[19] Dalmas de Réotier P and Yaouanc A 1994 *Phys. Rev. Lett.* **72** 290
[20] Henneberger S, Frey E, Maier P G, Schwabl F and Kalvius G M 1999 *Phys. Rev.* B **60** 9630
[21] Yaouanc A, Dalmas de Réotier P, Gubbens P C M, Mulders A M, Kayzel F E and Franse J J M 1996 *Phys. Rev.* B **53** 350
[22] Yaouanc A, Dalmas de Réotier P, Gubbens P C M, Kaiser C T, Menovsky A A, Mihalik M and Cottrell S P 2002 *Phys. Rev. Lett.* **89** 147001
[23] de Renzi R, Guidi G, Podini P, Tedeschi R, Bucci C and Cox S F J 1984 *Phys. Rev.* B **30** 197
[24] Frey E and Schwabl F 1994 *Adv. Phys.* **43** 577
[25] Yaouanc A, Dalmas de Réotier P and Frey E 1993 *Phys. Rev.* B **47** 796
[26] Dalmas de Réotier P, Yaouanc A and Frey E 1994 *Phys. Rev.* B **50** 3033
[27] Bak P and Jensen M H 1980 *J. Phys. C: Solid State Phys.* **13** L881
[28] Nakanishi O, Yanase A, Hasegawa A and Kataoka M 1980 *Solid State Commun.* **35** 995
[29] Vojta T and Sknepnek R 2001 *Phys. Rev.* B **64** 052404
[30] Chubukov A V, Pépin C and Rech J 2004 *Phys. Rev. Lett.* **92** 147003
[31] Semadeni F, Roessli B, Böni P, Vorderwisch P and Chatterji T 2000 *Phys. Rev.* B **62** 1083